From DMO to MZO:A Review

Dr. Jagmeet Singh

Geodata Processing and Interpretation Centre, ONGC Ltd., Dehradun, India

Summary

We review DMO processing techniques that have been in common practice in the industry. We introduce the reader to Zhang's DMO which is an improved version of Hale's DMO, and provides 'true' amplitude despite being kinematic in approach.We also discuss Migration to Zero Offset (MZO)which includes the NMO step used before DMO within the MZO operator.We carry out experiments with different DMO techniques and make a comparative study of aliasing noise and amplitudes obtained by these methods.

Introduction

We discuss, here, various approaches to DMO that have been in practice in the industry since its inception. We start with the t-x domain method of Deregowski &. Rocca (1981) followed by the method of Hale(1984) which works in the f-k domain. We introduce the reader to the more appropriate form of f-k DMO due to Zhang(1988) which is true amplitude in its nature. This is followed by a brief discussion of Migration to Zero Offset (MZO)(Popovici 1990) which includes the NMO step used before DMO within the MZO operator. We then give a brief description of the method of Hale(1991) for antiialiasing of t-x DMO. Finally, we discuss the results of our experiments on point diffractor(s), compare aliasing noise as well as amplitudes obtained by different DMO schemes, and give useful insights on the same.

We start with Fig. 1, where we show a dipping reflector OL at an angle θ w.r.t. the horizontal. The aim of the DMO program is to bring the NMOed data to its true zero offset position $\mathbf{y_0}$ (point P in fig. 1) with the correct zero offset time $\mathbf{t_0}$. Subsequent post stack time migration positions the data below point vertically above D, its true subsurface position.

The NMO equation is given as

$$t^2 = \frac{t_0'^2 + h^2\cos^2\theta}{v_{half}^2} \qquad (1)$$

where v_{half} is half the medium velocity, h is half-offset and t_0' is the zero offset time corresponding to the midpoint M, i.e. two times the time taken to traverse the perpendicular MF from point M to the dipping reflector. Note that t_0' is not the true zero offset time, the time corresponding to the perpendicular PD which we call t_0.

Deregowski and Rocca's DMO

Deregowski and Rocca's DMO works in t-x domain and uses a geometrical optics approach to calculate the DMO operator or the response of an impulse in a constant offset section mapped to zero offset .They first calculate the fully migrated output corresponding to the impulse i.e. they find

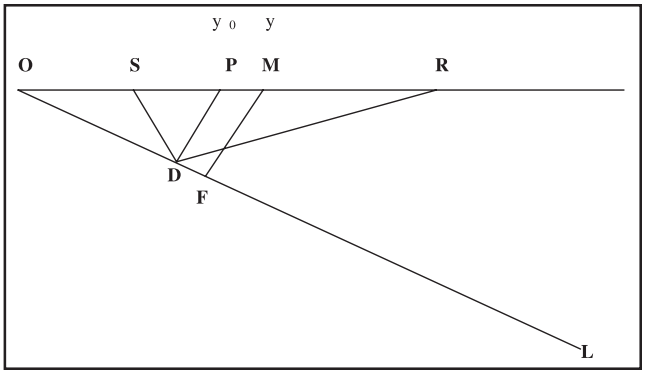

Fig.1.

the reflector that would have given rise to an impulse in the constant offset section; this is then used to find the zero offset response.

They start out with an impulse at $y = y_h$, $t = t_h$ in the (y, t) plane of a constant offset section where y is the midpoint and t is the two way time .The migrated output of this is clearly an ellipse, the locus of a point such that the time from the shot to the point to the geophone equals t_h. For $y_h = 0$, equation of this ellipse in the migrated (x', τ) plane, where τ is the one way time is given as

$$\frac{x'^2}{a^2} + \frac{\tau^2}{b^2} = 1 \qquad (2)$$

with a and b given as

$$a = v_{half}\, t_h$$

$$b = (1/2)\,[t_h^2 - h^2/v_{half}^2]^{1/2} = t_n/2, \qquad (3)$$

where t_n is the NMO corrected time. From each point (x, τ) on this elliptical reflector, we now draw a normal to the ellipse upto the surface, in order to get the zero offset coordinates (x,t). The point of intersection of the normal with the surface gives us x, whereas two way time t equals r/v_{half} , where r is the length of the normal. Figure 2 shows the zero offset section or the DMO impulse response obtained from the migration ellipse.Without deriving the equation for (x,t), we give the parametric equation for the DMO impulse response

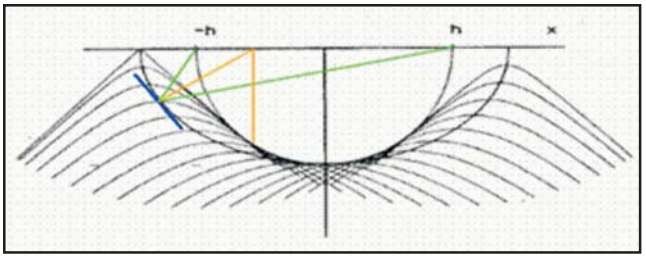

Fig.2. For a given source receiver pair,the travel time t_h is same for all points on the migration ellipse.Considering the migration ellipse as the reflector,construct a zero offset section.The outcome is the DMO impulse response.The zero offset point diffraction hyperbolae from all points on the migration ellipse, define the DMO impulse response.

$$x = h^2 \cos\phi / v_{half}\, t_h$$

$$t = t_n [\sin^2\phi + (t_n^2/t_h^2)\cos^2\phi]^{1/2}, \quad (4)$$

where ϕ is a parameter lying between $-\pi$ & π .The DMO smile is bounded according to the limits on ϕ. Clearly,x lies between $-x_m$ to x_m, where $x_m = h^2/v_{half}\, t_h$. The smile is a part of a larger ellipse with h and t_n as the semi-major and semi-minor axes respectively. Note that the velocity enters only through the aperture x_m. The DMO ellipse itself is velocity independent. Also note that the zero offset time that is achieved after the t-x DMO is t_0 (not t_0') . It can be shown that

$$t_0^2 = t_n^2 (1 - b^2/h^2), \quad (5)$$

where b is the distance PM in Fig. 1.

With the above background, the mapping defined by DMO may be written as

$$P_0(x,t) = \int\int P_h(y,t_h) \,.\, S(x-y,t,t_h)\, dy\, dt_h \quad (6a)$$

where

$$S(x,t,t_h) = L(x)\, \delta[t - t_n(1-x^2/h^2)] \text{ for } |x| < h^2/v_{half}\, t_h,\ t > 0. \quad (6b)$$

L(x) defines the amplitude distribution along the smile. The amplitude is taken to be proportional to the curvature of the elliptical reflector whence

$$L(x) \propto v t_n\, (1 - Ax^2)/2h^2 \quad (7)$$

with

$$A = \frac{3}{2h^2}\left[\frac{v^2 t_n^2}{4h^2} - 1\right]$$

Comparing equations (5) and (6),we see that the zero offset time one would get after the t-x DMO would be the correct zero offset time t_0 .

Hale's DMO

We start out by Fourier transforming the target data $p_0(t_0', y, h)$ corrected to time t_0', the zero offset time *corresponding to CMP y*, with offset h, as follows

$$P_0(\omega_0, k_y, h) = \int dt_0' \exp(i(\omega_0 t_0')) \int dy \exp(-ik_y y)\ p_0(t_0', y, h) \quad (8)$$

We now express the above Fourier transform in terms of the NMO corrected time t_n (see (3)) .Starting out with (1),we write t_0' in terms of t_n :

$$t_0' = [t_n^2 + h^2 \sin^2\theta / v_{half}^2]^{1/2} \quad (9)$$

It can be easily shown from the geometry of Fig. 1 that

$$\sin\theta = v_{half}\, (\delta t_0'/y), \quad (10)$$

so that (9) may be written as

$$t_0' = [t_n^2 + h^2 (\delta t_0'/\delta y)^2]^{1/2} \quad (11)$$

Defining

$$A = (dt_n/dt_0') = t_0'/t_n = [1 + (h^2/t_n^2) .(\delta t_0'/\delta y)^2]^{1/2} \quad (12)$$

And using (11) to replace $p_0(t_0,y,h)$ with $p_n(t_n,y,h)$, (8) becomes

$$P_0(\omega_0, k_y, h) = \int dt_n A^{-1} \exp(i(\omega_0 t_n A)) \int dy \exp(-ik_y y)\ p_n(t_n, y, h) \quad (13)$$

For a reflector with arrival times t_0', the slope $(\delta t_0'/\delta y)$ that occurs via A in (13) may be replaced by (k_y/ω_0). With this replacement, it becomes easy to evaluate the double integral and obtain $P_0(\omega_0, k_y, h)$.Now, one just needs to inverse Fourier Transform $P_0(\omega_0, k_y, h)$ to obtain $p_0(t_0', y, h)$.

Notice the difference in the zero offset times and the lateral positions used by Deregowski &. Rocca(viz. t_0, y_0) and that used by Hale(viz. t_0', y). Is this a source of problem? This is not a major problem, because as long as the data is moved to a point(y or y_0) with the 'zero offset time corresponding to the point', there is no error (in lateral or vertical positioning).The question above was examined in detail by Zhang(1988) and, to no surprise, their DMO operator had the same phase as that of Hale's. What was different, however, was the amplitude spectrum.

Before we go into the details of Zhang's result and its implications, let us examine Hale's DMO a bit more closely. At first glance, one may get the impression from (13) that there is only a vertical shift (and no lateral shift) in Hale's DMO. But , because of the presence of factor A(which in turn depends on k_y and ω_0),data at position y does not map onto output data at the same position y. Only if the slope k_y/ω_0 equals zero, the lateral as well as vertical shift is zero. In fact, using (13) one can find out the impulse response of

Hale's DMO. This was done by Hale(1991) and an outline of their derivation is given below.

Starting with an impulse $p_n(t_n, y, h) = \delta(t_n - T)\delta(y)$ in (13) we get

$$P_0(\omega_0, k_y, h) = \frac{\exp[i\omega_0 T\{1+ (h^2/T^2).(k_y/\omega_0)^2\}^{1/2}]}{\{1+ (h^2/T^2).(k_y/_0)^2\}^{1/2}} \qquad (14)$$

The above may be inverse Fourier transformed to get the impulse response. Cutting short the long calculation, we give the result. It is found that the impulse response lies primarily along the ellipse (under the approximation $\omega_0 t_0' >>1$):

$$(t_0'^2/t_n^2) + x^2/h^2 = 1\,, \qquad (15)$$

which is indeed the same ellipse as that of Deregowski & Rocca.

For the sake of completeness and without going into the details, we mention here that in most practical implementations, Hale's DMO is not used in the above form. One commonly employs logarithmic transformations (see e.g. Notfors & Godfrey 1987)) which render the DMO operator temporally and spatially invariant making the algorithm faster. We turn our attention to Zhang's DMO below.

Zhang's DMO

Taking into account the geometry in Fig. 1, it can be shown that

$$PM = y-y_0 = h^2 \sin\theta/v_{half}(t_n^2 + h^2\sin^2\theta/v_{half}^2)^{1/2} \qquad (16)$$

and

$$t_0 = t_n^2/(t_n^2 + h^2/v_{half}^2)^{1/2} \qquad (17)$$

where t_0 is the true zero offset time corresponding to y_0 i.e. point P. Following Hale, we Fourier transform the desired field $p_0(t_0, y_0, h)$

$$P_0(\omega_0, k_{y0}, h) = \int dt_0 \exp(i(\omega_0 t_0)) \int dy_0 \exp(-ik_{y0}y)\; p_0(t_0, y_0, h) \qquad (18)$$

The differentials dy_0 and dt_0 are given as

$$dy_0 = dy$$

$$dt_0 = dt_n \{t_n (t_n^2 + 2h^2/v_{half}^2)\}/(t_n^2 + h^2/v_{half}^2)^{3/2}\,, \qquad (19)$$

whereby (18) becomes

$$P_0(\omega_0, k_{y0}, h) = \int dt_n \int dy\, A^{-1} \{(t_n^2 + 2h\, k_{y0}^2/\omega_0^2)\}/(t_n^2 + h^2\, k_{y0}^2/\omega^2{}_0)\} \cdot p_n(t_n, y, h) \exp(i(\omega_0 t_n A) \exp(-ik_{y0}y), \qquad (20)$$

where A is as defined in (12) above. We note that the phase factor above is the same as in Hale's DMO , and that the only difference is in the Jacobians. Hale's Jacobian A^{-1} gets multiplied by the factor within curly brackets in the above equation.

Hale equates the DMO corrected amplitude $p_0(t_0', y, h)$ to the NMO corrected amplitude $p_n(t_n, y, h)$. But note that the two events are reflected from two different points for a dipping reflector. Hence Hale's operator does not preserve the correct amplitudes for events reflected from a dipping reflector. Zhang makes the correct assumption $p_0(t_0, y_0, h) = p_0(t_n, y, h)$ and thereby Zhang's DMO operator has uniform amplitude spectrum with repect to dips and offsets.

Interestingly, the results of Zhang based on a purely kinematic approach agree with those of Black and Egan(1988) who used the wave equation for obtaining their *true amplitude* DMO. By true amplitude we mean that the peak amplitude of a migrated event is proportional to the reflection coefficient. The problem of true amplitude DMO was examined in detail by Black et al. (1993). They calibrated the filter term that appears in integral(t-x) DMO with the aim of preserving the amplitudes of an arbitrary dipping reflector and showed the equivalence of this method (implemented in nonaliased fashion) with Zhang's f-k DMO. Fig. 3 shows a comparison of Hale's vs. Zhang's DMO on common offset sections obtained from a reflector with varying dips. Clearly amplitudes are better preserved in the case of Zhang's DMO.

MZO

As the name suggests, MZO or Migration to Zero Offset takes the data(at position y) directly to zero offset(at position y_0) bypassing the NMO step(rather including the NMO operation within the MZO operator).The transformation is now from $p_0(t_0, y_0, h)$ to $p(t_h, y, h)$. Starting from (18) above and using the following transformation(similar to (19))

$$dy_0 = dy$$
$$dt_0 = dt_h \{t_h(t_h^2 - h^2/v_{half}^2 + 2h^2k_{y0}^2/\omega_0^2)\}/(t_h^2 - h^2/v_{half}^2 + h^2k_{y0}^2/\omega_0^2)^{3/2} \qquad (21)$$

we obtain

$$P_0(\omega_0, k_{y0}, h) = \int dt_h \int dy\, \{t_h (t_h^2 - h^2/v_{half}^2 + 2h^2\, k_{y0}^2/\omega_0^2)\}/(t_h^2 - h^2/v_{half}^2 + h^2\, k_{y0}^2/\omega_0^2)^{3/2} \cdot p(t_h, y, h) \exp\{i(\omega_0(t_h^2 - h^2/v_{half}^2 + h^2\, k_{y0}^2/\omega_0^2)^{12}\} \exp(-ik_{y0}y)$$

$$= \int dt_h \{t_h (t_h^2 - h^2/v_{half}^2 + 2h^2\, k_{y0}^2/\omega_0^2)\}/(t_h^2 - h^2/v_{half}^2 + h^2\, k_{y0}^2/\omega_0^2)^{3/2} \cdot p(t_h, k_{y0}, h) \exp\{i(\omega_0(t_h^2 - h^2/v_{half}^2 + h^2\, k_{y0}^2/\omega_0^2)^{12}\} \qquad (22)$$

We note again that the phase above is the same as that of Hale and Zhang while the Jacobian above (which we call J_M) is related to Zhang's Jacobian (J_Z) as follows.

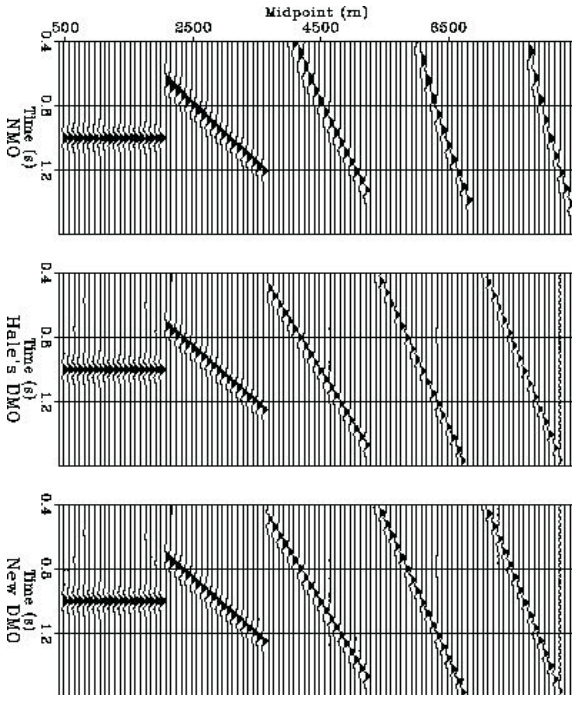

Fig. 3. This figure is taken from from Lin Zhang's article on DMO in SEP report #70.Common offset sections are shown.Top: after NMO correction; middle: after Hale's DMO correction; bottom: after Zhang's DMO correction. The offset is 2000 meters,and the dips of the reflectors are 0, 20, 40, 60, 80 degrees. Notice the difference in amplitudes of the two DMO schemes.

$$J_M / J_Z = (1 + h^2/t_n^{\,2}\, v_{half}^{\,2})^{1/2} \qquad (23)$$

which corresponds to the Jacobian of the NMO transformation.

Relevance of DMO

The main advantage of MZO/DMO is the accuracy in lateral positioning of the reflected energy. The DMO impulse response is not very sensitive to errors in the NMO time shift[8] and insensitive to errors in velocity(as we discussed above, the DMO ellipse is independent of velocity). If we talk in terms of requirements of velocity accuracy for different migration schemes, the velocity accuracy required for MZO is the least whereas depth migration requires the highest accuracy [9].Although, with availability of high computing power, pre-stack time migration (PSTM) is now routinely used, DMO/MZO should be preferred when velocity accuracy is low.

Even when PSTM is used, DMO followed by inverse NMO and fresh velocity analysis provides one a good starting point for the r.m.s. velocities to be used in PSTM. We may add here that for constant velocity case, MZO equals NMO plus Zhang's DMO, but for variable velocity media the two are not equivalent and that is where MZO scores over DMO[10]. We should also add here that , even though, Common Reflection Surface(CRS) method proposed recently[11] is a better alternative to DMO, the more recent Output Imaging Scheme of CRS stack uses DMO as an intermediate step[12].

Antialiasing of t-x DMO

Before we can discuss the results of some of the experiments that we have carried out, it is important to discuss the problem of spatial aliasing of Deregowski and Rocca's tx DMO impulse response. Even for a horizontal reflector, precursor noise(noise above the horizontal reflector time) is seen. This is due to aliasing of high frequencies in the dipping portions of the DMO ellipse and non-cancellation of the resulting amplitudes above the reflector time. The amplitudes fail to cancel as the time shift of the waveform from one trace to another, in the impulse response, exceeds one half-cycle.

The problem was addressed by Hale(1991) and his solution is briefly discussed below. In the usual t-x DMO one generates, from a non-zero offset trace, a number of zero offset traces at times t_0 and position x according to the following equation

$$t_0 = t_n(1-x^2/h^2)\,, \qquad (24)$$

where t_n is the NMO corrected time. Hale implements this equation in a different way. The input trace is first shifted in time by say

$$\delta t = t_n - t_0 \qquad (25)$$

and then mapped on to an x given as

$$x = \pm h\{\delta t/\, t_n(2 - \delta t/\, t_n)\}^{1/2} \qquad (26)$$

Equation (26) is equivalent to (24).A succession of such time shifts are applied and mapped to the corresponding x. To eliminate spatial aliasing, time shifts are not allowed to exceed the time sampling interval and the difference in these time shifts is adjusted so that x's don't differ by more than one CMP interval.

Results and Discussion

We now discuss the results of some of the experiments that we have carried out on a point diffractor and a reflector. A flat top hyperbola generated from a point diffractor in common offset is expected to change to a sharper zero offset hyperbola after NMO+DMO(see Fig. 4). As is well known, these hyperbolae are sections of Cheops pyramid, a 3D plot of time vs. midpoint and offset for the case of a point diffractor. Fig. 5(a) shows a constant/common offset(2000m) section obtained from a point diffractor, at a depth of 1000m, in a medium with velocity 2000m/s and Fig. 5(b) shows the zero offset section obtained from such a diffractor.

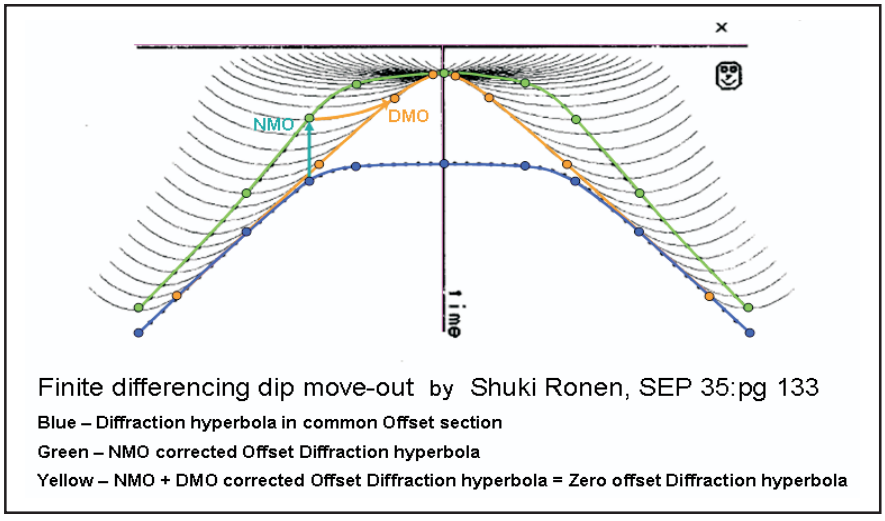

Fig. 4.

Fig. 6 shows a comparison of three different DMO schemes applied to the section in Fig. 5(a).Fig. 6(a) shows the result of nonaliased t-x DMO due to Hale, whereas 6(b) shows the result (Notfors and Godfrey's version) of Hale's f-k DMO and 6(c) shows the result of Deregowski and Rocca's t-x DMO. A lot of noise is seen around the apex of the hyperbola, especially in Fig. 6(c).This noise results from crowding of energy/amplitudes near the apex (apparent from Fig. 4) and failure of these amplitudes to cancel, in regions beyond the target zero offset time, *mainly* due to aliasing of the DMO impulse responses (in case of t-x DMO of Deregowski and Rocca).Note that the ellipses arriving at the apex originate *mostly* from the horizontal portions of the NMOed hyperbola(though this would vary), leading to the conclusion that aliasing of DMO ellipses is the *chief* cause of aliasing noise near the apex. As explained in the previous section, the amplitudes fail to cancel as time shift from one trace to another, in an impulse response, exceeds half a cycle.

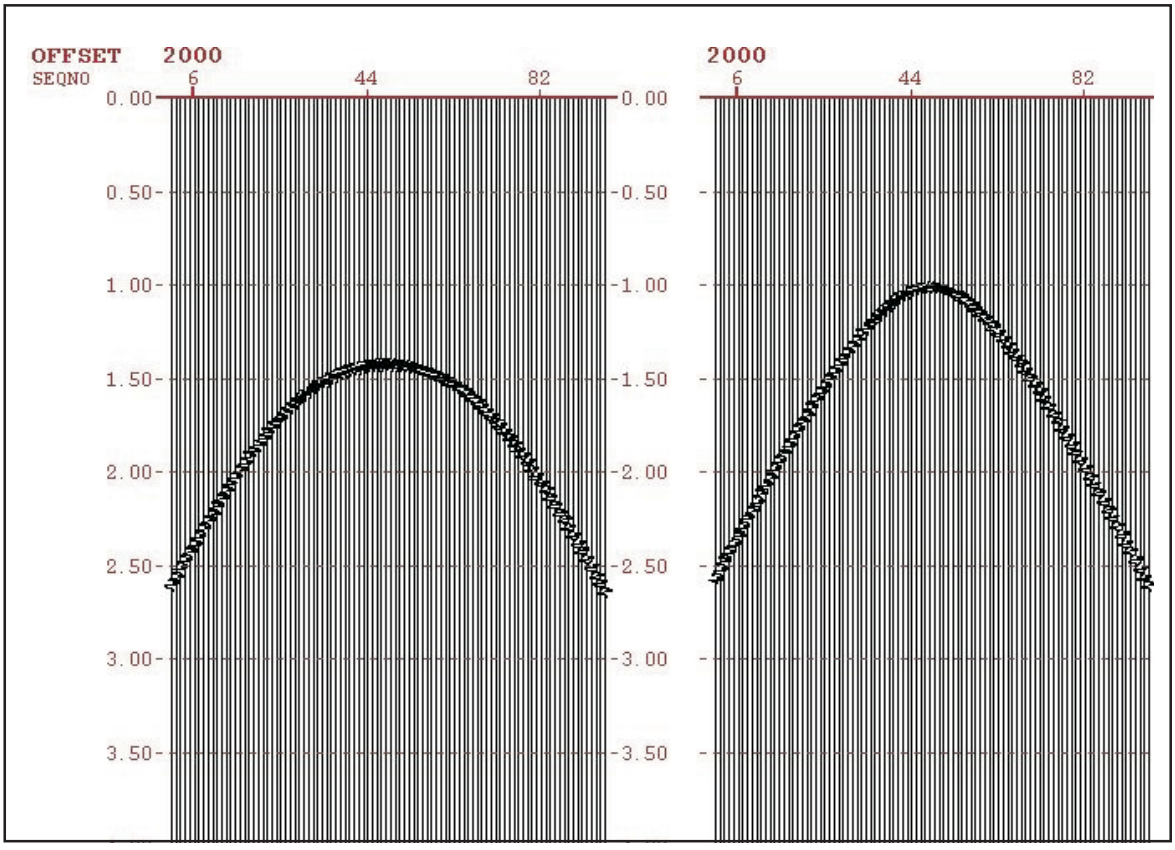

(a) Point diffractor:common offset(2000m)
Note that the hyperbola here has a flat top.

(b)Point diffractor:zero offset

Fig. 5.

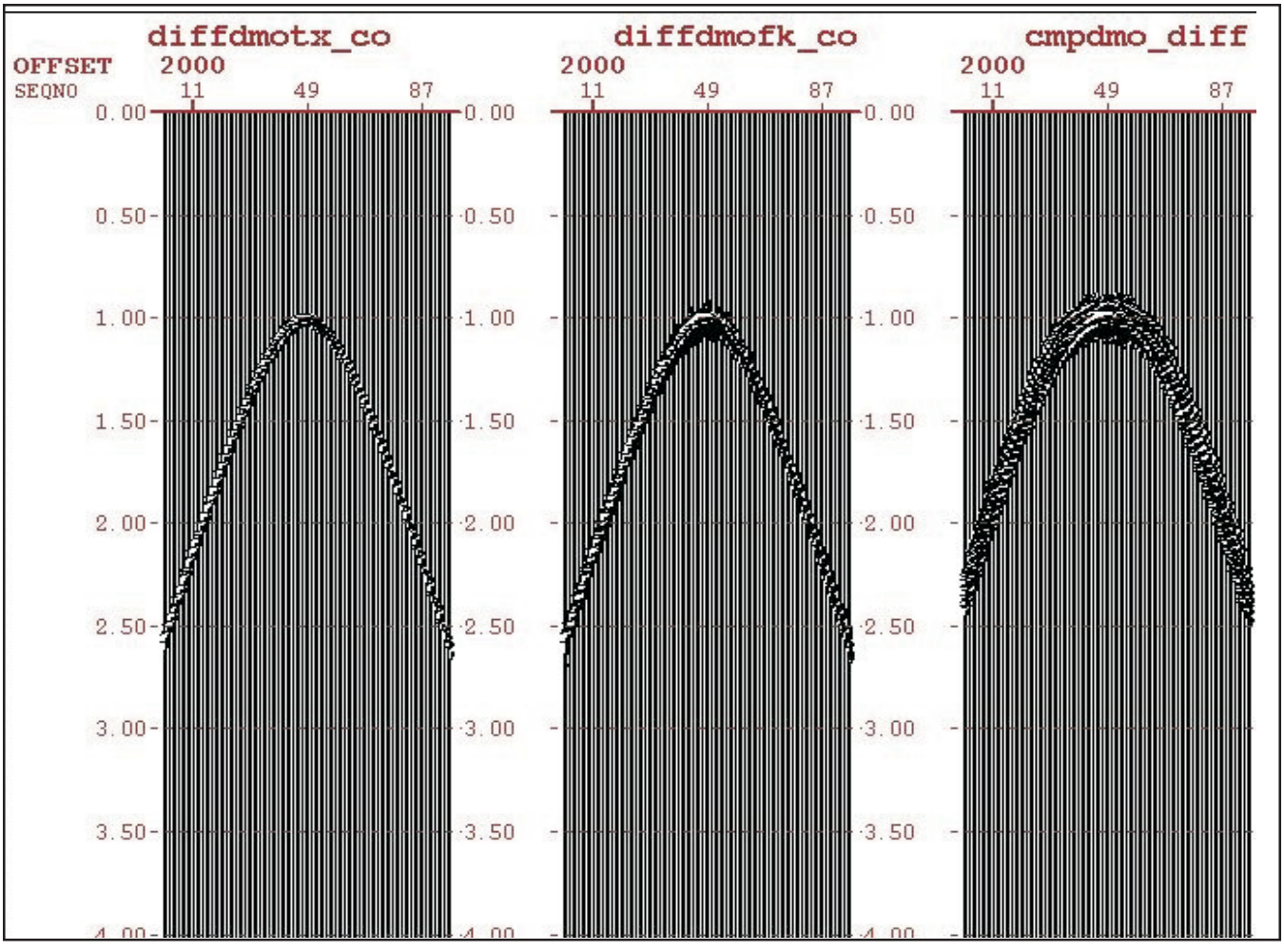

(a) (b) (c)

Fig. 6. Comparison of different DMO schemes applied to common offset section in fig. 5(a)
(a):NMO+ t-x DMO(antialiased version due to Hale)
(b):NMO+ (Notfors & Godfrey's version of) Hale's f-k DMO
(c):NMO + t-x DMO of Deregowski & Rocca.

The aliasing is higher near the apex as bigger DMO ellipses and hence higher dips (of these ellipses) come into play in this region, as is clear from Fig. 4.

Aliasing noise is, of course, also seen in the dipping portions of the hyperbolae. This is due to two reasons, namely aliasing of high frequencies in the dipping portions as well as in the slant portions of the DMO ellipses. The latter becomes less and less important as we go down the hyperbola since DMO action decreases and ellipses get smaller with increasing time . Hale's nonaliased version of t-x DMO, which differs from t-x DMO of Deregowski and Rocca in only the aliasing aspect of the DMO operator, has worked well(Fig. 6a) in removing the aliasing noise. Hale's f-k DMO too has less of aliasing noise as it attenuates the high frequencies that would be aliased at the steep flanks of the DMO response.Aliasing in DMO outputs can also be reduced by reducing the CMP interval or by trace interpolation as Fig. 7 shows.

Fig. 8a shows a common offset(2000m) section of horizontal reflector at depth of 1000m in a medium of velocity 2000m/s.Fig. 8b shows the output of Hale's nonaliased t-x DMO.Fig 8c shows the output of Hale's DMO and fig. 8d that of Deregowki and Rocca's DMO.Fig. 8c shows ,interestingly, that whatever noise remains near the apex in Fig. 6(b) has been attenuated due to contributions from neighbouring point diffractors, that are there in case of a reflector.This suggests that non-cancellation of amplitudes near the apex for f-k dmo in fig. 6(b) is not only due to aliasing but also because there are no neighbouring point diffractors to contribute the canceling amplitudes. Fig. 8d shows a lot of undesirable precursor noise arising due to reasons discussed above.

Having discussed aliasing noise, we now turn our attention to amplitudes. In Fig. 9, we compare the amplitudes that we obtained after Hale's f-k DMO and Hale's nonaliased t-x DMO for the point diffractor discussed above. We find Hale's f-k DMO and his nonaliased t-x DMO are at par as far as amplitude 'reponse' is concerned. Spherical divergence

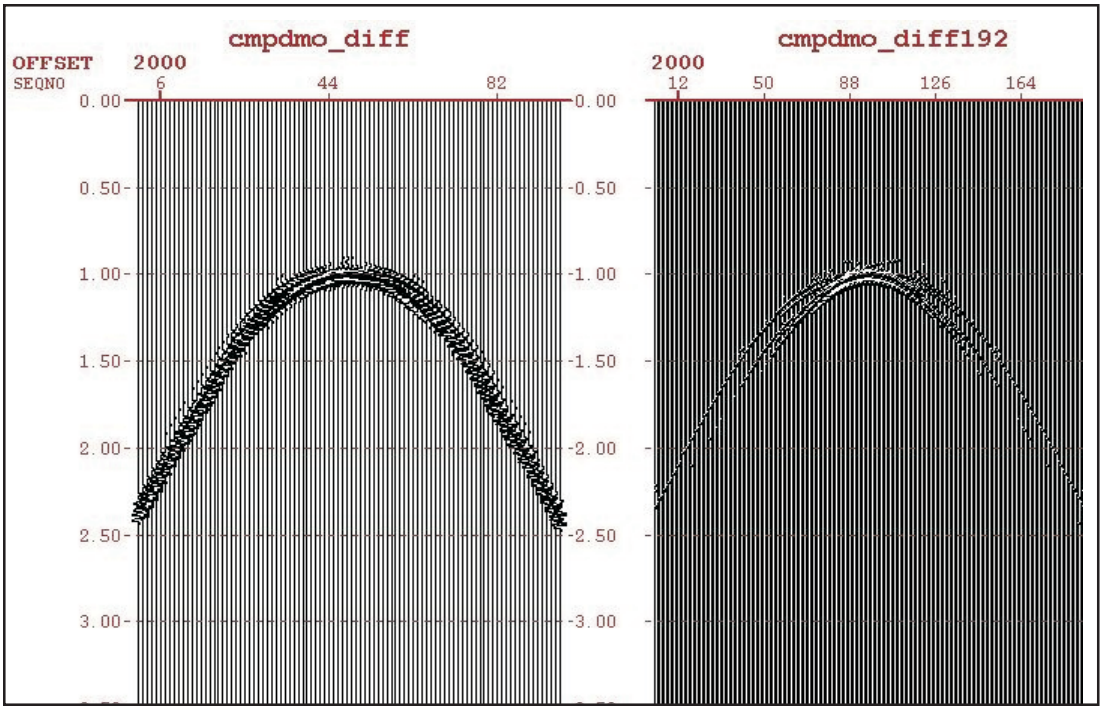

(a) (b)

Fig. 7.(a) : Deregowski & Rocca's t-x DMO output with CMP interval equal to 50m. **(b)**: with CMP interval 25m.

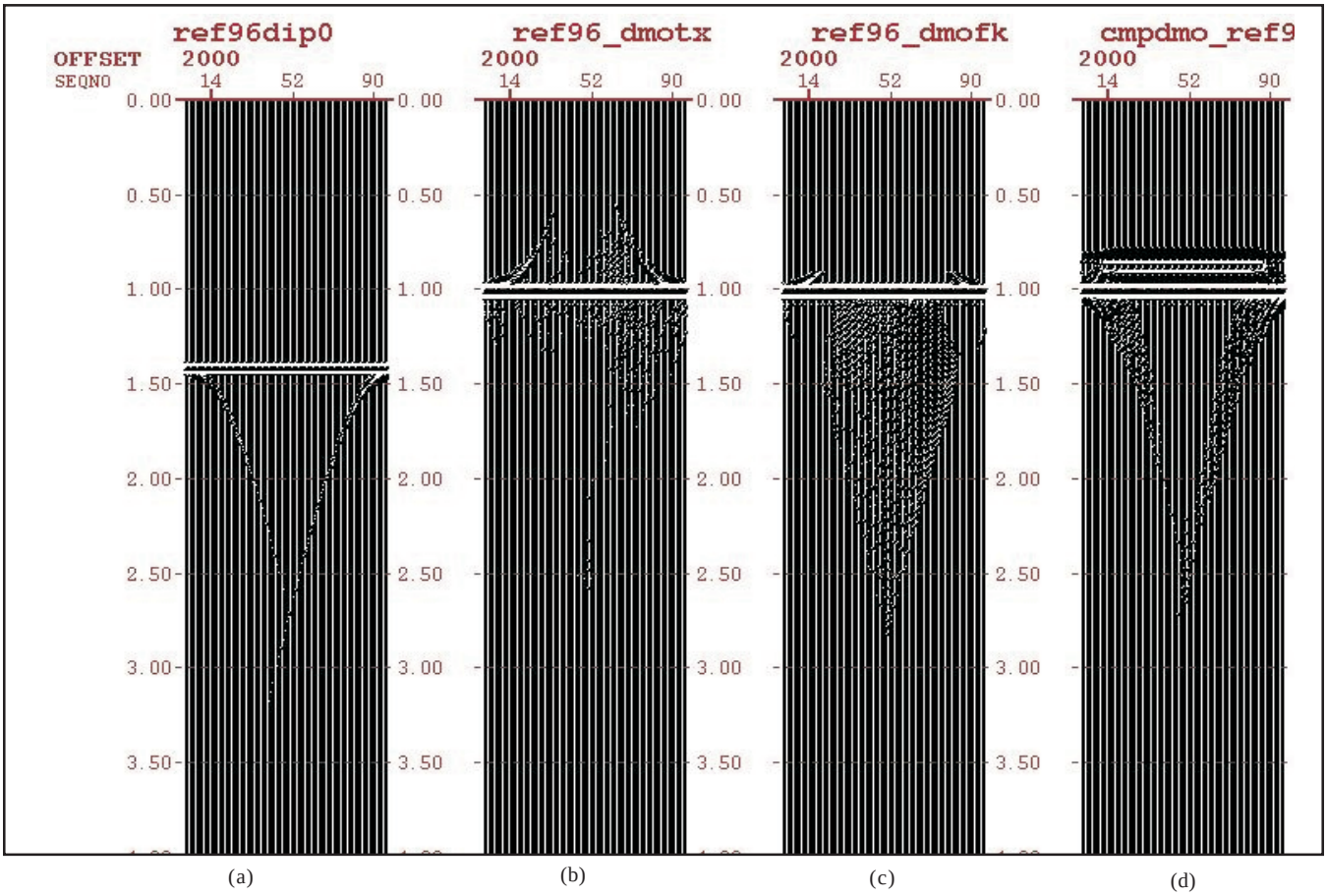

(a) (b) (c) (d)

Fig. 8. Fig. 8a shows input common offset(2000m) data with a horizontal reflector. Fig. 8b shows the result obtained from nonaliased t-x dmo due to Hale.Fig. 8c shows the output of f-k dmo of (Notfors & Godfrey's version) of Hale's DMO whereas Fig. 8d shows the result obtained from t-x DMO of Deregowski & Rocca.

correction leads to further improvement in the output amplitudes(Fig. 9(b)).Fig. 10 shows the amplitudes of the same point diffractor with trace interval four times that in Fig. 9.We see a clear deterioration in the amplitude response. Spatial aliasing not only leads to the aliasing noise discussed above, but also has a harmful effect on the amplitudes.

What really are we looking for in an amplitude response of DMO for a point diffractor? The shape of the amplitude curve should be close to the original. A reflector may be looked upon as a series of closely spaced point diffractors. If the amplitude response of DMO outputs(for all point diffractors) is just a scaled down version of the original, the relative amplitudes for reflectors are preserved(which is what we really mean by true amplitude). Black et al.(1993) compared the amplitudes of Zhang's, Hale's f-k DMO and t-x DMO for a dipping reflector and showed that (in case of Hale's f-k DMO and t-x DMO) for a given dip, amplitudes fall off with offset and for a given offset, the amplitudes fall off with dip. This is also reflected in Fig. 3 , where amplitudes are seen to get weak with increasing dip, in case of Hale's DMO (unlike Zhang's DMO).Spherical divergence correction was applied in all cases in Black et. al's study. This dip and offset dependent behaviour may be linked to the mismatch of shapes of the output amplitude curves with that of the original.

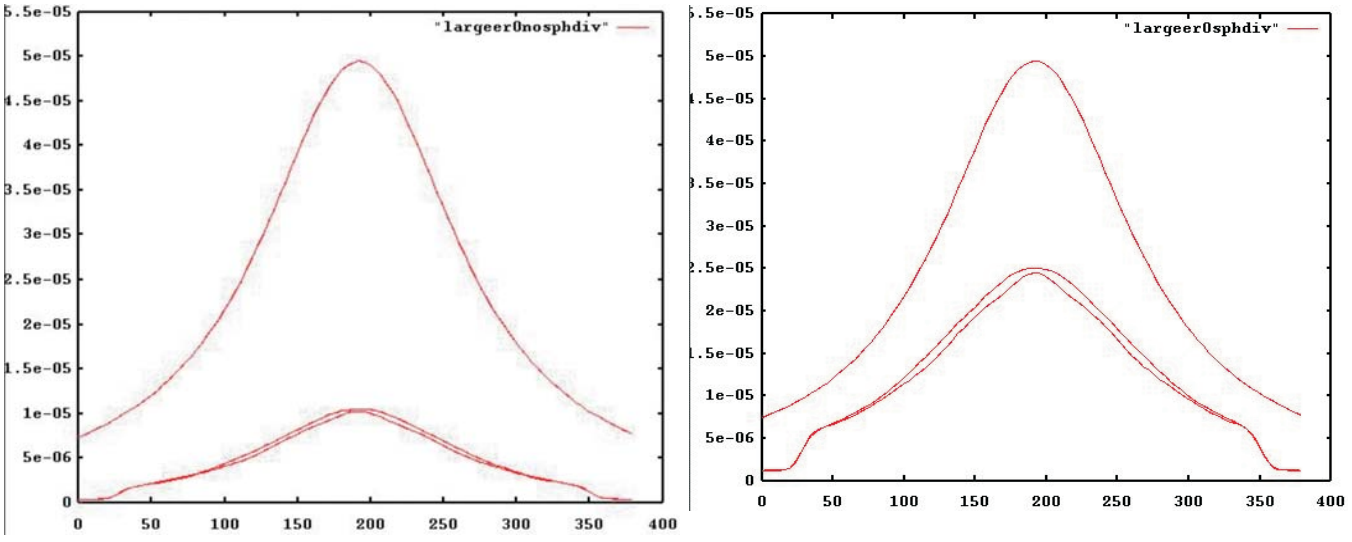

Fig. 9. A comparison of amplitudes obtained by f-k DMO of Hale and nonaliased t-x DMO.
9(a) : topmost curve shows amplitudes along the original (target) zero offset hyperbola, bottom curves : amplitudes along outputs of Hale's nonaliased t-x dmo and fk DMO after NMO.
9(b) : same as 9(a) except that prior to NMO and DMO,spherical divergence correction is applied.

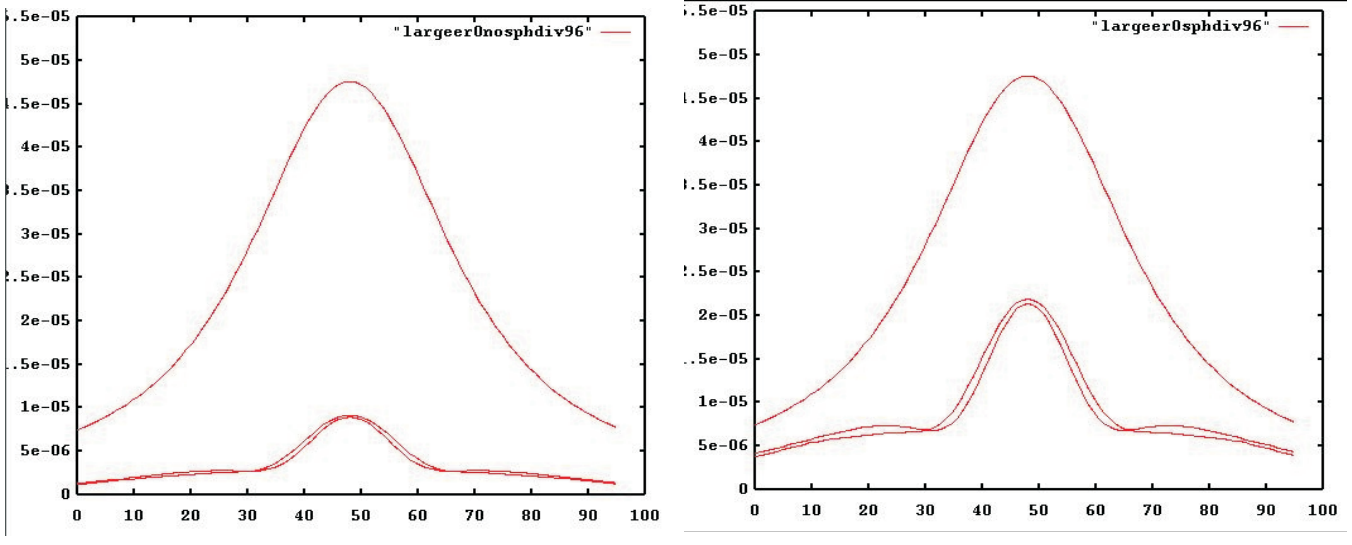

Fig. 10. Comparison of amplitudes: Trace interval is 4 times that in Fig. 9.
10(a) : topmost curve shows amplitudes along the original (target) zero offset hyperbola, bottom curves : amplitudes along outputs of Hale's nonaliased t-x dmo and fk DMO after NMO.
10(b) : same as 10(a) except that prior to NMO and DMO,spherical divergence correction is applied.

Conclusions

We have covered in the present review, commonly used kinematic or ray-theoretic approaches to DMO. We have made a comparison of their advantages and disadvantages. We have discussed the superiority of Zhang's DMO over Hale's DMO, to MZO. We have discussed the issues of aliasing noise and (true) amplitude in DMO. We have carried out experiments, using different methods, on a point diffractor and made a comparative study of aliasing noise and amplitudes obtained by these methods. In particular, we have shown that, although, Hale's nonaliased t-x DMO is somewhat better than his f-k DMO in tackling aliasing noise, the two are at par in preserving amplitude. We have given a criterion for judging the true amplitude nature of DMO. We have shown that spatial aliasing has a harmful effect on amplitudes.Finally, some of the concepts developed here are not only restricted to DMO, but extend to all (prestack) migration schemes.

Acknowledgements

I am grateful to Shri S.K. Das, GGM (Geophy(S)), Head Geopic, and Shri K. Neogy, GM(Geophy(S)),Head(Proc.), Geopic for their encouragement and support during this work. I express my sincere thanks to Shri T.R. Murali Mohan,DGM(Geophy(S)) for introducing me to SEG's publication 'DMO Processing' ,which had all the relevant papers at one place. I am indebted to Dr. C.H. Mehta, retd. ED(Prog.), ex-Head(Geopic) and Dr. J.V.S.S.N. Murty, Chief Geophy(S) for useful suggestions which led to an improvement in the amplitude figures and overall presentation of the paper.

References

Deregowski S.M. and Rocca F. 1981.Geometrical Optics and Wave Theory of Constant Offset Sections in Layered Media, Geophysical Prospecting,29,374-406.

Hale Dave1984. Dip-moveout by Fourier Transform, Geophysics, 49,741-757.

Zhang Lin 988.A New Jacobian for Dip-moveout,Stanford Exploration Project report number 59 ; J.L. Black,K.L. Schleicher and L. Zhang 1993 : True amplitude imaging and dip moveout, Geophysics, 58, 47-66.

Popovici A.M. 1993.DMO and MZO Amplitudes,Stanford Exploration Project Report number 77.

Hale Dave 1991.A Nonalised Method for Dip-moveout,Geophysics,56,795-805.

Notfors C.D. and Godfrey R.J. 1987.Dip-moveout in the Frequency Wavenumber Domain,52,1718-1721.

Black L.J.and Egan S.E. 1988.True Amplitude DMO in 3D,presented at the 58th SEG Annual International Meeting in Anaheim.

Deregowski S.M. 1986.What is DMO?, First Break, 4, 7-24 .

Höcht G., Hubral P., Perroud H. 1997.Migrating Aound on Hyperbolas and Parabolas, The Leading Edge 16, 473-476.

Popovici A.M. 1991.Migration to Zero Offset in Variable Velocity Media, Stanford Exploration Project Report number 70.

Jaiger R.,Mann J.,Hocht G. and Hubral P.2001.Common Reflection Surface Stack:Image and Attributes,Geophysics 66, 97.

Yang K., Wang H.Z. and L.G. Dong L.G. 2006.Output Imaging Scheme of the Common Reflection Surface Stack:Applications to Real Data,SEG/New Orleans 2006 Annual Meeting.